HHS Public Access

Author manuscript

Part Part Syst Charact. Author manuscript; available in PMC 2016 August 01.

Published in final edited form as:

Part Part Syst Charact. 2015 August ; 32(8): 809–816. doi:10.1002/ppsc.201500025.

A Biomimetic Core-Shell Platform for Miniaturized 3D Cell and Tissue Engineering

Pranay Agarwal,
Department of Biomedical Engineering, The Ohio State University, Columbus, OH 43210 (USA). Dorothy M. Davis Heart and Lung Research Institute, The Ohio State University, Columbus, OH 43210 (USA)

Dr. Jung Kyu Choi,
Department of Biomedical Engineering, The Ohio State University, Columbus, OH 43210 (USA). Dorothy M. Davis Heart and Lung Research Institute, The Ohio State University, Columbus, OH 43210 (USA)

Haishui Huang,
Department of Biomedical Engineering, The Ohio State University, Columbus, OH 43210 (USA). Dorothy M. Davis Heart and Lung Research Institute, The Ohio State University, Columbus, OH 43210 (USA). Department of Mechanical and Aerospace Engineering, The Ohio State University, Columbus, OH 43210 (USA)

Shuting Zhao,
Department of Biomedical Engineering, The Ohio State University, Columbus, OH 43210 (USA). Dorothy M. Davis Heart and Lung Research Institute, The Ohio State University, Columbus, OH 43210 (USA)

Jenna Dumbleton,
Department of Biomedical Engineering, The Ohio State University, Columbus, OH 43210 (USA). Dorothy M. Davis Heart and Lung Research Institute, The Ohio State University, Columbus, OH 43210 (USA)

Prof. Jianrong Li, and
Department of Veterinary Biosciences, The Ohio State University, Columbus, OH 43210 (USA)

Prof. Xiaoming He[*]
Department of Biomedical Engineering, The Ohio State University, Columbus, OH 43210 (USA). Dorothy M. Davis Heart and Lung Research Institute, The Ohio State University, Columbus, OH 43210 (USA). Comprehensive Cancer Center, The Ohio State University, Columbus, OH 43210 (USA)

Abstract

[*]he.429@osu.edu.
PA and JKC contributed equally to this work.

Supporting Information
Supporting Information is available from the Wiley Online Library or from the author.

This article describes a biomimetic core-shell platform with a collagen-based core and an alginate hydrogel shell for cell and tissue culture. With this system, chemical and physical properties of extracellular matrix (ECM) in the core microenvironment can be controlled to regulate proliferation and development of cells/tissues under miniaturized three-dimensional (3D) culture.

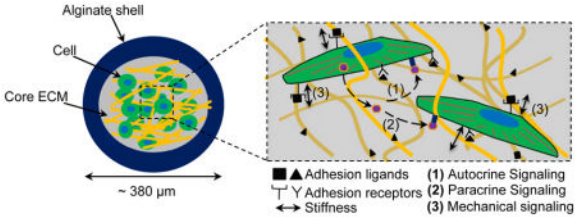

Keywords

biomimetic; core-shell microcapsule; 3D culture; stem cell; follicle

Cells and tissues interact dynamically with the physical and chemical cues present in their microenvironment including the insoluble extracellular matrix (ECM) and soluble endocrine, paracrine, and autocrine cytokines, which determines the morphology, differentiation, proliferation, development, and function of the cells and tissues.[1–6] A number of methods have been developed to control the cell and tissue microenvironment *in vitro* by patterning adhesive proteins/peptides (e.g., fibronectin/RGD) on two-dimensional (2D) substrates (e.g., glass and plastic) with various physical and chemical properties.[7–9] Although it has contributed significantly to the understanding of cell/tissue biology, 2D culture differs substantially from the *in vivo* microenvironment of most cells and tissues where they are intricately associated with various adherent ligands present on three-dimensional (3D) ECM.[1,10–13] Therefore, studies have been reported to encapsulate/embed cells and tissues in homogeneous 3D ECM made of one or more natural/synthetic polymers such as alginate, collagen, hyaluronic acid, polyethylene glycol (PEG), and polycaprolactone for *in vitro* culture.[12,14–19] However, most of the reported 3D ECMs are macroscale (at least in millimeters) scaffolds where many cells/tissues may suffer hypoxia and/or deprivation of nutrients because the diffusion length of oxygen and nutrients in cellularized tissue is usually less than ~200 μm.[1,20,21] To overcome this problem, encapsulation of cells/tissues in sub-millimeter constructs (e.g., microcapsules or sheets) for 3D culture is attracting more and more attention. However, current effort in this regard has been focused on producing homogeneous microscale constructs, which does not recapitulate the heterogeneous nature of most cells/tissues/organs that usually have a central core for performing specific function(s) and an outer shell/wall that physically isolates the core from the surroundings.[22–24] For example, the plasma membrane of a cell helps to maintain intracellular concentrations of proteins and ions; the epidermis of skin helps to retain moisture in the tissues and organs semi-enclosed in it; the pericardium envelops the heart from the adjacent organs; and the zona pellucida that houses totipotent-pluripotent stem cells in pre-hatching embryos during early embryo development. In other words, both the central core and outer shell probably serve their purposes to maintain homeostasis in the cells/

tissues/organs. Indeed, our recent studies show that a liquid core semi-enclosed in a hydrogel shell is better than the conventional 2D culture on a substrate and 3D culture in homogeneous microscale hydrogel for maintaining stemness.[25–27] We also showed that ovarian preantral follicles cultured in a softer core semi-enclosed in a harder shell could develop better than the follicles under the conventional 2D and homogeneous 3D culture conditions.[28] However, the effect of the core ECM on the proliferation and development of the cells/tissues under the miniaturized 3D culture has not been rigorously studied. Here, we describe the encapsulation of mouse embryonic stem cells (mESCs) and ovarian preantral follicles (with vastly different ECMs in their native niches *in vivo*) in the bio-inspired microcapsules comprised of a protein or protein-based (instead of liquid) core and hydrogel shell, which allows precise control of the microenvironment to modulate the cell/tissue proliferation and development under the miniaturized biomimetic 3D culture.

We used naturally occurring alginate and type I collagen to fabricate the hydrogel shell and core of the microcapsules, respectively. Alginate was used due to its excellent biocompatibility and reversible gelation with divalent cations such as Ca^{2+} or Ba^{2+} under gentle conditions.[25–28] The alginate shell acts as an outer/surface layer that provides sufficient mechanical strength/structural support to maintain the integrity of the softer core ECM. Further, the nano-porous structure (pore size on the order of tens of nanometers[29,30]) of alginate shell may help to retain important autocrine and paracrine cytokines produced by encapsulated cells and tissues in the core ECM (i.e., reducing their dilution in the bulk medium). In brief, this biomimetic miniaturized 3D platform 1) ensures effective transport oxygen and nutrients due to their small size, 2) facilitates cell-cell contacts and autocrine and paracrine signals as a result of the miniaturized and semi-enclosed space, and 3) enables control of cell-ECM interactions by tuning the properties of core ECM.

We utilized high throughput microfluidic technique to encapsulate cells and tissues in the biomimetic core-shell microcapsules. Figure 1A shows a schematic illustration of the microfluidic device that consists of four inlets (I1, I2, I3, and I4) for injecting mineral oil emulsified with aqueous calcium chloride solution (Ca^{2+} oil emulsion), sodium alginate solution, ice-cold collagen-based solution (with or without cells/tissues), and aqueous extraction solution, respectively. At the flow-focusing junction (Figure 1B), the alginate (shell) and collagen (core) solutions were pinched off into spherical droplets by the Ca^{2+} oil emulsion as a result of interfacial tension. Alginate in the outer or shell layer of the spherical droplets was further gelled to form hydrogel when flowing in the serpentine channels by Ca^{2+} in the oil emulsion. Since an extended stay of microcapsules in the oil emulsion is harmful to the encapsulated cells (see Supplementary Figure S1 which demonstrates that on-chip extraction of microcapsules significantly increases the cell viability), we incorporated an extraction channel in the device to extract the core-shell microcapsules from the oil phase into aqueous phase based on intrinsic interfacial tension between water and oil,[31] as shown in Figure 1C. The aqueous phase containing microcapsules and the oil emulsion were collected from outlet O1 and O2, respectively. Microcapsules formed for the purpose of this study have a total and core size of 380.9 ± 33.98 μm and 285.05 ± 80.4 μm in diameter, respectively. The flow rates of solutions in the device can be easily varied to control the size of the microcapsules. The collected microcapsules were then incubated at 37 °C for 30 min

to crosslink collagen in the microcapsule core and cells/tissues in the microcapsules will be cultured for up to 10 days to monitor their proliferation and development (Figure 1D).

The 3D ECM can be tuned to modulate the cell proliferation, adhesion, and differentiation by using adhesion and signaling ligands and/or changing its structural/mechanical properties. We sought to investigate this by varying the concentration of collagen in the ECM between 0.5–5.0 mg ml^{-1}. We also incorporated, in some cases, alginate to the core ECM to further increase the mechanical properties of the ECM. To visualize and examine the fibrous structure of the ECM, we utilized differential interference contrast (DIC) and confocal reflectance microscopy (CRM) techniques. Figure 2A–D shows clearly the presence of collagen fibers in the core ECMs of the microcapsules. Furthermore, we quantified two structural parameters (fiber length and width) of different core ECMs in the microcapsules using CRM images. Our data indicate that as the concentration of collagen is increased, individual fibers become significantly thicker, longer, and more sparse (Figure 2E and Supplementary Figures S2–3). We further measured the viscoelastic properties including both storage (G′, representing elastic effect) and loss (G″, representing viscous effect) modulus of core ECMs made of either single component (0.5–5.0 mg ml^{-1} collagen) or two components (a mixture of 5.0 mg ml^{-1} collagen and 5.0 mg ml^{-1} alginate). As shown in Figure 2F, by increasing the collagen concentration in core ECM, we were able to regulate G′ between 0.48 and 429.74 Pa and G″ between 1.14 Pa and 68.45 Pa. More detailed frequency sweep graphs for the viscoelastic properties of the different core ECMs are provided in Supplementary Figure S4.

After determining the effects of collagen concentration on fiber structure and mechanical properties of the core ECM in the core-shell microcapsules, we encapsulated mESCs in the different core ECMs to investigate their effect on the cell proliferation and pluripotency. Since stem cells naturally reside in a soft/liquid microenvironment, we chose 0.5 mg ml^{-1} ($G' < G''$), 1.5 mg ml^{-1} ($G' \approx G''$), and 3.0 mg ml^{-1} ($G' > G''$) for our experiments. We suspended mESCs at a density of 5×10^6 cells ml^{-1} in ice-cold collagen (0.5, 1.5, and 3.0 mg ml^{-1}) solution and injected the cell suspension into the core channel (I3) of the microfluidic device (Figure 1) to form microcapsules. Collected microcapsules (containing 48 ± 11 cells per microcapsule) were then cultured in stem cell culture medium for up to 10 days. Figure 3A–F shows the typical phase contrast and corresponding live/dead staining fluorescence images of stem cell aggregates formed on day 10 in different collagen ECMs and the corresponding quantitative data of the aggregate size are given in Figure 3G. As it is evident from the data, we observed the formation of a single large aggregate in each microcapsule with ECM made of low concentrations of collagen (313.1 ± 75.8 and 293.61 ± 102.8 μm for 0.5 and 1.5 mg ml^{-1}, respectively) and significantly smaller aggregates (128.1 ± 51.9 μm) in the ECM made of 3.0 mg ml^{-1}collagen. Supplementary Figure S5 shows the phase contrast images of mESCs proliferating in different core ECMs on days 1, 5, and 10. These data indicate that the mESCs exhibit high proliferation in microenvironment with the low adhesion and soft ECM. This is possibly because the lower adhesion and softer ECM better mimics the permissive proteinaceous microenvironment in the core semi-enclosed in a hydrogel-like shell (known as the zona pellucida) of a pre-hatching embryo and enhances the pluripotency of the cells,[25,26] we further sought to investigate the effect of the different core ECMs of collagen on the cell stemness. To do this, we conducted quantitative RT-PCR

studies for the expression of four pluripotency genes (Oct-4, Sox2, Nanog, and Klf2). The data shown in Figure 3H indicate that as the adhesion ligand/elastic modulus of the encapsulating ECM increases (from 0.5 mg ml^{-1} to 3.0 mg ml^{-1}), the expression of three pluripotency markers (Sox2, Klf2, and particularly Nanog) significantly decreases. Possibly, culturing mESCs in liquid or soft ECM ($G' < G''$) of 0.5 mg ml^{-1} collagen facilitates e-cadherin mediated cell-cell interactions, which enhances the self-renewal capacity of mESCs (therefore bigger aggregates) through up-regulation of Sox2, Nanog, and Klf2.[32,33] On the other hand, the increase in ligand density and stiffness of the ECM facilitates mechanical interactions between the ECM and mESCs *via* integrins on the cells, which favors differentiation as suggested by the down-regulation of pluripotent gene markers.[32,33] Moreover, it is worth noting that although the aggregate size is not significantly different for the 0.5 and 1.5 mg ml^{-1} collagen core ECMs, the gene expression could be significantly different. Therefore, proliferation alone may not be a good indicator of a culture condition for maintaining the cell properties. All in all, these data indicate that biological characteristics of mESCs can be easily regulated in this biomimetic culture system.

Furthermore, to encapsulate small tissues in this miniaturized system, we chose preantral follicles (at the early secondary stage and with a diameter of 100–135 μm) obtained from deer mice (deer mice are more suitable for research aimed for medical applications due to its outbred nature similar to humans).[28,34] Follicles are the fundamental tissue unit of mammalian ovary and each preantral follicle consists of one single oocyte that is surround by layered granulosa and theca cells (Supplementary Figure S6).[28,34] By providing necessary chemical and mechanical cues, the preantral follicle can be developed to an antral stage to obtain fertilizable oocytes, which may help to restore/preserve fertility in women.[28,34] *In vivo* proliferation of preantral follicles occurs in collagen rich medullar region of the ovaries. Therefore, to study the effect of ECMs on follicle development, we encapsulated the follicles in three types of core ECMs: 1.0 mg ml^{-1} collagen, 5.0 mg ml^{-1} collagen, and a mixture of 5.0 mg ml^{-1} collagen and 5.0 mg ml^{-1} alginate to significantly vary ligand concentration and mechanical properties (G' between: 1.42 and 429.74 Pa and G'' between: 2.49 and 68.45 Pa) of the ECMs. Also, we chose 5.0 mg ml^{-1} ECM core as a baseline based on the findings in a previous study.[28] Typical bright field images showing the encapsulated early secondary preantral follicle in 5 mg ml^{-1} collagen ECM are shown in Supplementary Figure S7.

In our experiments, we observed 24.4% (11/45) development of preantral follicles to the antral stage after 10 days culture in the 5.0 mg ml^{-1} collagen core ECM (Figure 4A). By contrast, development of follicles to the antral stage remarkably decreased to 2.6% (1/38) when the concentration of collagen was lowered to 1.0 mg ml^{-1}. Interestingly, when the structural and mechanical properties of the core ECM were changed while keeping the number of adhesion ligands the same (in 5.0 mg ml^{-1} collagen) by adding 5.0 mg ml^{-1} alginate (see Figure 2E–F), we also observed lower (10.8%) development of follicles into the antral stage (Figure 4A and Supplementary Table S1). Representative DIC and live/dead images showing the morphology and high viability of cells in the antral follicle at day 10 are given in Figure 4B and C, respectively. Figure 4D shows the DIC image of an antral follicle released from the microcapsule together with the oocyte and fluid-filled antral cavity in the

follicle. Typical images showing proliferation and development of the encapsulated early secondary preantral follicle to the antral stage in the three types of ECMs are given in Supplementary Figure S8. The corresponding quantitative data showing proliferation (diameter of follicles) of the preantral follicles (that did develop to the antral stage excluding those became degenerated) at 1, 6, 8, and 10 days of culture in the core ECMs are shown in Figure 4E, which indicates slightly (but insignificantly) higher proliferation in the 5.0 mg ml^{-1} collagen ECM compared to the other two.

We further analyzed the production of estradiol (Figure S6) in follicles (at days 1, 8 and 10) which is essential for the regulation of estrous and menstrual reproductive cycles of females.[35] The data (Figure 4F) indicate a significant increase in estradiol secretion at day 10 compared to day 8 in all the encapsulating ECMs. Moreover, we observed significantly higher production of estradiol in 5.0 mg ml^{-1} collagen ECM than the other two ECMs. Higher estradiol concentration from antral follicles encapsulated in the 5.0 mg ml^{-1} collagen ECM indicates better quality of antral follicles. To affirm the quality of developed antral follicles, we performed *in vitro* maturation (IVM) of the cumulus-oocyte complex (Supplementary Figure S6) from the antral follicles. Although none of the oocytes in the antral follicles cultured in the other two ECMs (0/1 and 0/4, 0%) developed to the metaphase II (MII) stage, we obtained 5 MII oocytes out of the 11 antral follicles (45.5%) cultured in 5.0 mg ml^{-1} collagen core ECM (Supplementary Table S1). We hypothesize that as the growing follicle expands inside the microcapsules, it experiences mechanical stresses from the surrounding core ECM that is communicated rapidly throughout the follicle. The ECM made of 5 mg ml^{-1} collagen probably provides an optimum mechanical and chemical microenvironment essential for proliferation, differentiation, and development of the encapsulated follicles. Other formulations of ECM provide minimal (1.0 mg ml^{-1} collagen) or excessive (5.0 mg ml^{-1} alginate in 5.0 mg ml^{-1} collagen) mechanical stresses that inhibit development of follicles. The ECM of 1.0 mg ml^{-1} collagen could be insufficient in cell adhesion ligand density for the encapsulated follicle to develop and proliferate either as the adhesion ligand density (involved in secretion of estradiol) and the mechanical properties of the ECM play an equally important role in regulating follicle development.[36,37] In addition, these data together with that in Figure 4E–F indicate that proliferation alone may not be a good indicator of a culture condition for maintaining tissue properties. A typical DIC image of the MII oocytes obtained is shown in Figure 4G. To further confirm the developmental stage of the MII oocytes, we stained the meiotic spindles and nuclei by tubulin (in microtubules of the spindles) antibody and Hoechst, respectively. Figure 4H shows the ordered attachment of meiotic spindles (green) to the chromosomes (blue) in the cytoplasm while the arrangement of tubulin and chromosomes is chaotic in the first polar body, which is characteristic of MII oocytes. It is worth noting that only MII oocytes could be further activated or fertilized into embryos for further embryonic development. Therefore, we used 3 of the MII oocytes to obtain early embryos by parthenogenetic activation, for which we successfully obtained one 2-cell stage embryo (Figure 4I). Overall, these data suggest that development of preantral follicles is sensitive to cell adhesion ligand density as well as the mechanical properties of the ECM under biomimetic 3D culture.

Cells and tissues respond to subtle changes in their microenvironment that is known to affect its proliferation, morphology, adhesion, migration, differentiation, and development. This paper describes a novel approach to engineer the cellular and tissue microenvironment and control its biological impact by encapsulating cells/tissues in biomimetic 3D core-shell microcapsules where core and shell are composed of biocompatible/natural collagen and alginate, respectively. The collagen core can be easily replaced with other biocompatible synthetic or natural polymers. Our data show that proliferation alone is not sufficient to judge the quality of cells/tissues under biomimetic 3D culture. We anticipate this 3D biomimetic platform will find its broad applications in many fields including but not limited to regenerative medicine, developmental biology, and high throughput drug screening.

Experimental Section

See Supplementary Information for details on fabrication of microfluidic device, cell culture, animal care and use, isolation of preantral follicles, and preparation of mouse embryonic fibroblasts (MEFs).

Generation of core-shell microcapsules in non-planar microfluidic device

The fluids in the shell (from I2 entrance) and core (from I3 entrance) microchannels were purified sodium alginate (2%, Sigma) and collagen solution (BD Bioscience), respectively. To minimize the mixing of core and shell solutions during microcapsule formation, we increased the viscosity of the core solution by adding 1% sodium carboxymethyl cellulose (Sigma) to the collagen mix while keeping the final collagen concentration between 0.5–5.0 mg ml^{-1}. For the separation channel (from I4 entrance), 1% sodium carboxymethyl cellulose solution was used which was necessary for maintaining a stable interface between oil and aqueous phase[31]. All the solutions (except collagen solution that is phosphate-buffered according to the manufacturer's instructions) were sterile and buffered with 10 mM HEPES to maintain pH 7.2 before use. Further, osmolality of all the solutions were maintained at 300 mOsm by the addition of D-Mannitol (Sigma). To make mineral oil infused with aqueous calcium chloride solution for flowing in the oil channel (from I1 entrance), stable emulsion of mineral oil and 1.0 g ml^{-1} aqueous calcium chloride solution (volume ratio: 5:1 with the addition of 1.2% SPAN 80) was prepared by sonication for 1 min using a Branson 450 Sonifier. All solutions (except collagen that was kept at ice temperature) were injected into the microfluidic device using syringe pump (Pump 11 Elite, Harvard Apparatus) at room temperature (RT) to generate microcapsules in oil phase and then extract them to aqueous phase. Flow rates for core, shell, oil, and aqueous extraction fluid were 100 μl hr^{-1}, 250 μl hr^{-1}, 6 ml hr^{-1}, and 4 ml hr^{-1}, respectively. Outlets of the device were connected to 50 ml centrifuge tube containing appropriate medium for each cell or tissue. Microcapsules were collected and the collagen core further gelled at 37 °C for 30 min in the incubator.

Encapsulation of cells and follicles

A neutralized collagen solution (2x) was prepared according to manufacturer's instruction (BD Bioscience) by mixing the stock collagen solution with appropriate volumes of NaOH, 10x PBS, and DI water. The solution was kept at RT for 10 min to initiate pre-gelling. After 10 min, cells and 2% sodium carboxymethyl cellulose were added to the collagen solution

on ice. Final collagen concentration and cell density in the core solution were 0.5–3.0 mg ml^{-1} and 5×10^6 cells ml^{-1}, respectively. Similar method was applied to encapsulate preantral follicles except that the concentration of collagen in the core solution was 1.0–5.0 mg ml^{-1}. In addition, in some cases we added 5.0 mg ml^{-1} alginate to the core solution to further tune the mechanical properties of the core ECM. Encapsulated cells/follicles were collected and cultured in their respective medium at 37 °C in a humidified 5% CO_2 incubator.

In vitro culture of encapsulated mESCs and pluripotency analysis

Encapsulated mESCs were cultured in their culture medium (see Supplementary Methods for medium composition) for 10 days. On day 10, mESC aggregates were released from the core-shell microcapsules with 75 mM sodium citrate (~5 min to dissolve alginate), followed by 1000 units ml^{-1} type I collagenase (30 min at 37 °C to remove the collagen ECM). Aggregates were then washed with PBS, pipetted several times to make them single cells and then centrifuged. RNAs were extracted from the aggregated cells using RNeasy plus mini kit (Qiagen, Valencia, CA) following the manufacturer's instruction. Next, reverse transcription was carried out to generate complementary DNA (cDNA) using the iScript™ cDNA synthesis kit (Bio-Rad, Hercules, CA) and GeneAmp 9700 PCR system. Quantitative RT-PCR was conducted with the superfast SYBR Green mix (Bio-Rad) using a Bio-Rad CFX96 real time PCR system. Pluripotency genes Oct-4, Sox2, Nanog, and Klf2 were studied with GAPDH being used as the housekeeping gene. Primer sequences of GAPDH and the pluripotency genes are given in Table S2.

In vitro culture of encapsulated preantral follicles and analysis of hormone release

Encapsulated preantral follicles were cultured (one in each well) in 100 μl of follicle culture medium (see Supplementary Methods for follicle culture medium composition) on MEFs feeder (cell density: 2×10^4 cells/well) in 96-well plate. On the following day, 100 μl of fresh medium was added to each well. Starting from day 3, half of the medium (100 μl) was replaced with fresh medium every other day till day 10. The replaced medium (100 μl) was collected and used to analyze estradiol (E2) with an estradiol EIA Kit according to the manufacturer's instruction (Cayman). Colorimetric analysis was conducted with a microplate reader (PerkinElmer, Waltham, MA) at 405 nm.

In vitro maturation (IVM) of antral follicles and developmental competence of MII oocytes

For IVM, antral follicles on day 10 after liquefying alginate hydrogel using 75 mM sodium citrate were incubated for 48 h in 500 μl of α-minimum essential medium-glutamax medium supplemented with 1000 IU ml^{-1} mouse leukemia inhibitory factor (LIF), 5 μg ml^{-1} epidermal growth factor (EGF), 10 mg ml^{-1} streptomycin sulfate, 75 mg ml^{-1} penicillin G, and 5% (v/v) heat-inactivated fetal bovine serum (FBS) covered with 250 μl of mineral oil in a 4-well plate at 37 °C in 5% CO_2 air. After maturation, the cumulus–oocyte complex (COC) in each antral follicle was retrieved mechanically by follicular puncture. Oocytes were then released from the COC by incubating in hyaluronidase (200 IU mL^{-1}) for 2 min. Quality of the metaphase II (MII) oocytes was evaluated first by the extrusion of the first polar body and were stained to check meiotic spindle of microtubules. For the latter, MII

oocytes were fixed in 4% formaldehyde/PBS for 30 min at room temperature. The oocytes were then permeabilized and blocked in 1x PBS containing 0.5% Triton X-100 and 3% fetal bovine serum for 1 h at room temperature, followed by overnight incubation with diluted (1:200) monoclonal anti-α-tubulin antibody (Sigma) in the blocking solution at 4 °C. Samples were then washed for 1 h in blocking solution and incubated with 1:200 diluted AlexaFluor® 488 rabbit anti-mouse IgG (H + L) secondary antibody (Invitrogen) for 1 h at room temperature. Samples were further washed for 1 h in blocking solution and the cell nuclei stained for 20 min with Hoechst 333232 (1 μg ml^{-1}). After washing 3 times in 1x PBS, images were taken using a Zeiss (Oberkochen, Germany) microscope with a 40x oil objective. Quality of the MII oocytes was further assessed by their embryonic development after parthenogenetic activation using Ca^{2+}-free KSOM medium supplemented with 10 mM $SrCl_2$ and 5 μg ml^{-1} cytochalasin B for 3.5 h.

Rheological characterization of core and shell materials

Rheological measurements were carried out using 40 mm cone geometry plate on a TA Instrument AR-1000N rheometer. Neutralized collagen solutions at different concentrations were prepared as aforementioned and placed directly on the rheometer at 4 °C. Temperature was then raised to 37 °C for 30 min to gel the collagen. Stress sweeps at a constant frequency of 1 Hz were first performed to obtain the linear viscoelastic region for collecting subsequent data. Frequency sweeps were performed in the linear viscoelastic regimen to determine values of the storage/elastic (G′) and loss/viscous (G″) modulus. Values at 1 Hz are reported in Figure 2 for comparison of the different core ECMs.

Supplementary Material

Refer to Web version on PubMed Central for supplementary material.

Acknowledgments

This work was partially supported by grants from NSF (CBET-1033426) and NIH (R01EB012108).

References

1. Vunjak-Novakovic G, Scadden DT. Cell Stem Cell. 2011; 8:252. [PubMed: 21362565]
2. Engler AJ, Sen S, Sweeney HL, Discher DE. Cell. 2006; 126:677. [PubMed: 16923388]
3. Chen W, Villa-Diaz LG, Sun Y, Weng S, Kim JK, Lam RH, Han L, Fan R, Krebsbach PH, Fu J. ACS nano. 2012; 6:4094. [PubMed: 22486594]
4. Kshitiz, Hubbi ME, Ahn EH, Downey J, Afzal J, Kim DH, Rey S, Chang C, Kundu A, Semenza GL, Abraham RM, Levchenko A. Sci Signal. 2012; 5
5. Discher DE, Janmey P, Wang YL. Science. 2005; 310:1139. [PubMed: 16293750]
6. Beningo KA, Dembo M, Wang YL. Proceedings of the National Academy of Sciences of the United States of America. 2004; 101:18024. [PubMed: 15601776]
7. Khademhosseini A, Langer R, Borenstein J, Vacanti JP. Proceedings of the National Academy of Sciences of the United States of America. 2006; 103:2480. [PubMed: 16477028]
8. Kam L, Boxer SG. Journal of biomedical materials research. 2001; 55:487. [PubMed: 11288076]
9. Lin CC, Co CC, Ho CC. Biomaterials. 2005; 26:3655. [PubMed: 15621256]
10. Lutolf MP, Gilbert PM, Blau HM. Nature. 2009; 462:433. [PubMed: 19940913]

11. Cukierman E, Pankov R, Stevens DR, Yamada KM. Science. 2001; 294:1708. [PubMed: 11721053]
12. Tayalia P, Mendonca CR, Baldacchini T, Mooney DJ, Mazur E. Adv Mater. 2008; 20:4494.
13. Chan CY, Huang PH, Guo F, Ding X, Kapur V, Mai JD, Yuen PK, Huang TJ. Lab Chip. 2013; 13:4697. [PubMed: 24193241]
14. Chen AA, Sang V, Albrecht DR, Bhatia SN. BioMEMS and Biomedical Nanotechnology. 2007:23.
15. Collins MN, Birkinshaw C. Carbohyd Polym. 2013; 92:1262.
16. Glowacki J, Mizuno S. Biopolymers. 2008; 89:338. [PubMed: 17941007]
17. Liu CZ, Xia ZD, Han ZW, Hulley PA, Triffitt JT, Czernuszka JT. Journal of biomedical materials research Part B, Applied biomaterials. 2008; 85:519.
18. Dhandayuthapani B, Yoshida Y, Maekawa T, Kumar DS. Int J Polym Sci. 2011
19. Khetan S, Burdick JA. Biomaterials. 2010; 31:8228. [PubMed: 20674004]
20. Vunjak-Novakovic G, Tandon N, Godier A, Maidhof R, Marsano A, Martens TP, Radisic M. Tissue Eng Part B Rev. 2010; 16:169. [PubMed: 19698068]
21. Figallo E, Cannizzaro C, Gerecht S, Burdick JA, Langer R, Elvassore N, Vunjak-Novakovic G. Lab Chip. 2007; 7:710. [PubMed: 17538712]
22. Marieb, EN.; Hoehn, K. Human anatomy & physiology. Pearson; 2013.
23. Mitchell, B.; Sharma, R. Embryology: an illustrated colour bood text. Churchill Livingston-Elsview; 2005.
24. Lewis, R.; Graddin, D.; Hoefnagels, M.; Parker, B. Life. McGraw-Hill Higher Education; 2004.
25. Agarwal P, Zhao S, Bielecki P, Rao W, Choi JK, Zhao Y, Yu J, Zhang W, He X. Lab Chip. 2013; 13:4525. [PubMed: 24113543]
26. Zhao S, Agarwal P, Rao W, Huang H, Zhang R, Liu Z, Yu J, Weisleder N, Zhang W, He X. Integrative Biology. 2014; 6:874. [PubMed: 25036382]
27. Rao W, Zhao S, Yu J, Lu X, Zynger DL, He X. Biomaterials. 2014; 35:7762. [PubMed: 24952981]
28. Choi JK, Agarwal P, Huang H, Zhao S, He X. Biomaterials. 2014; 35:5122. [PubMed: 24702961]
29. Boontheekul T, Kong HJ, Mooney DJ. Biomaterials. 2005; 26:2455. [PubMed: 15585248]
30. Gillette BM, Jensen JA, Wang MX, Tchao J, Sia SK. Adv Mater. 2010; 22:686. [PubMed: 20217770]
31. Huang H, He X. Applied Physics Letters. 2014; 105:143704, 5. [PubMed: 25378709]
32. Chowdhury F, Li Y, Poh YC, Yokohama-Tamaki T, Wang N, Tanaka TS. PloS one. 2010; 5:e15655. [PubMed: 21179449]
33. Kim MH, Kino-oka M. Biomaterials. 2014; 35:5670. [PubMed: 24746960]
34. Choi JK, Agarwal P, He X. Tissue Eng Part A. 2013; 19:2626. [PubMed: 23789595]
35. Caligioni CS. Current protocols in neuroscience. Crawley, Jacqueline N., et al.2009Appendix 4 Appendix 4I
36. Woodruff TK, Shea LD. Reproductive sciences. 2007; 14:6. [PubMed: 18089604]
37. Woodruff TK, Shea LD. Journal of assisted reproduction and genetics. 2011; 28:3. [PubMed: 20872066]

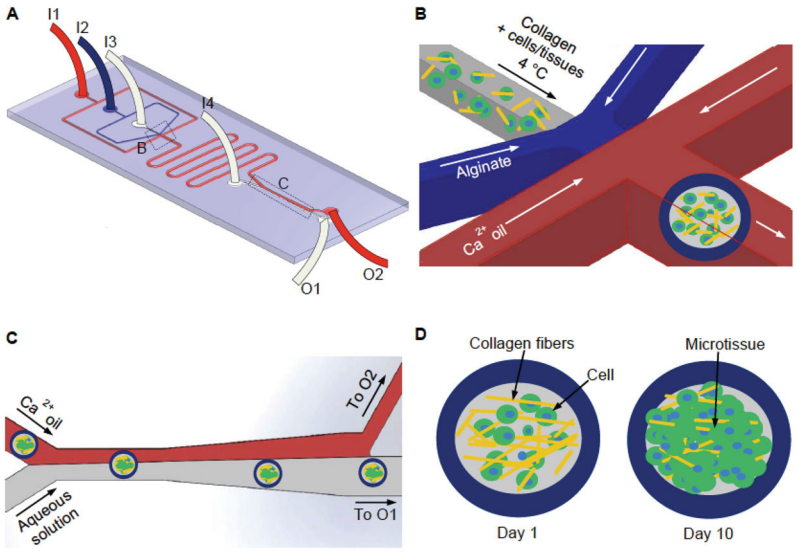

Figure 1.

A schematic illustration of the flow-focusing microfluidic device for encapsulating cells/tissues in the collagen-based core of microcapsules with an alginate hydrogel shell. (A) An overview of the microfluidic device showing Ca^{2+} oil, 2% sodium alginate, collagen (with or without cells), and aqueous extraction solutions were pumped into the device from inlets I1, I2, I3, and I4 respectively. The aqueous and oil phases exited the device from outlet O1 and O2, respectively. (B) A zoom-in view of the nonplanar flow-focusing junction where cells/tissues were encapsulated. (C) A zoom-in view of the channel where microcapsules in oil were extracted into aqueous phase. (D) Encapsulated cells/tissues were cultured for up to 10 days to form grown 3D microtissue.

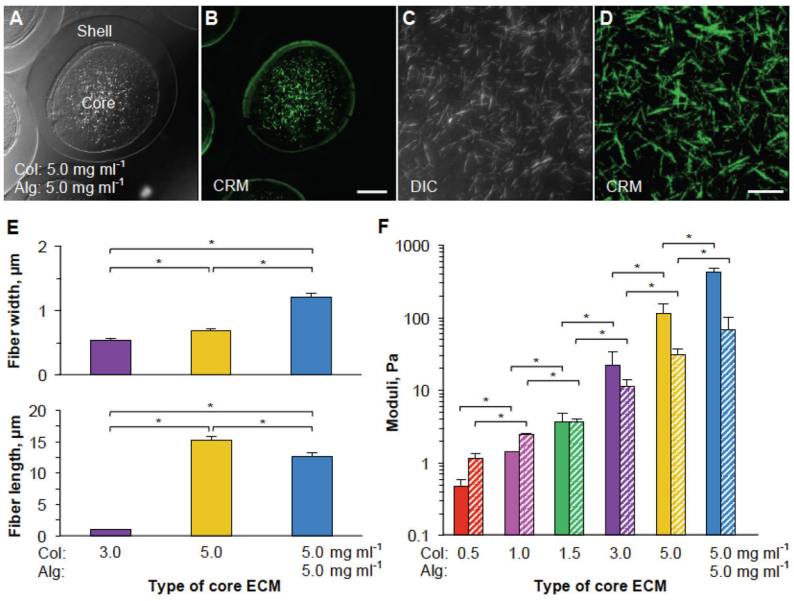

Figure 2.

Characterization of structural and mechanical properties of the core ECMs. (A–B) Typical differential interference contrast (DIC) and confocal reflectance microscopy (CRM) images of core-shell microcapsules with a core ECM made of 5.0 mg ml^{-1} collagen and 5.0 mg ml^{-1} alginate and a shell made of 2% (i.e., 20 mg ml^{-1}) alginate. (C–D) Higher magnification DIC and CRM images showing the fiber in the core ECM made of 5.0 mg ml^{-1} collagen and 5.0 mg ml^{-1} alginate. (E) Quantitative data of fiber length and width of different core ECMs. (F) Mechanical properties (storage moduli, G′ and loss moduli, G″ shown as solid and patterned bars, respectively) of different core ECMs. Col: collagen. Alg: alginate. * denotes $p < 0.05$. Scale bar: 100 μm in A and B and 20 μm in C and D.

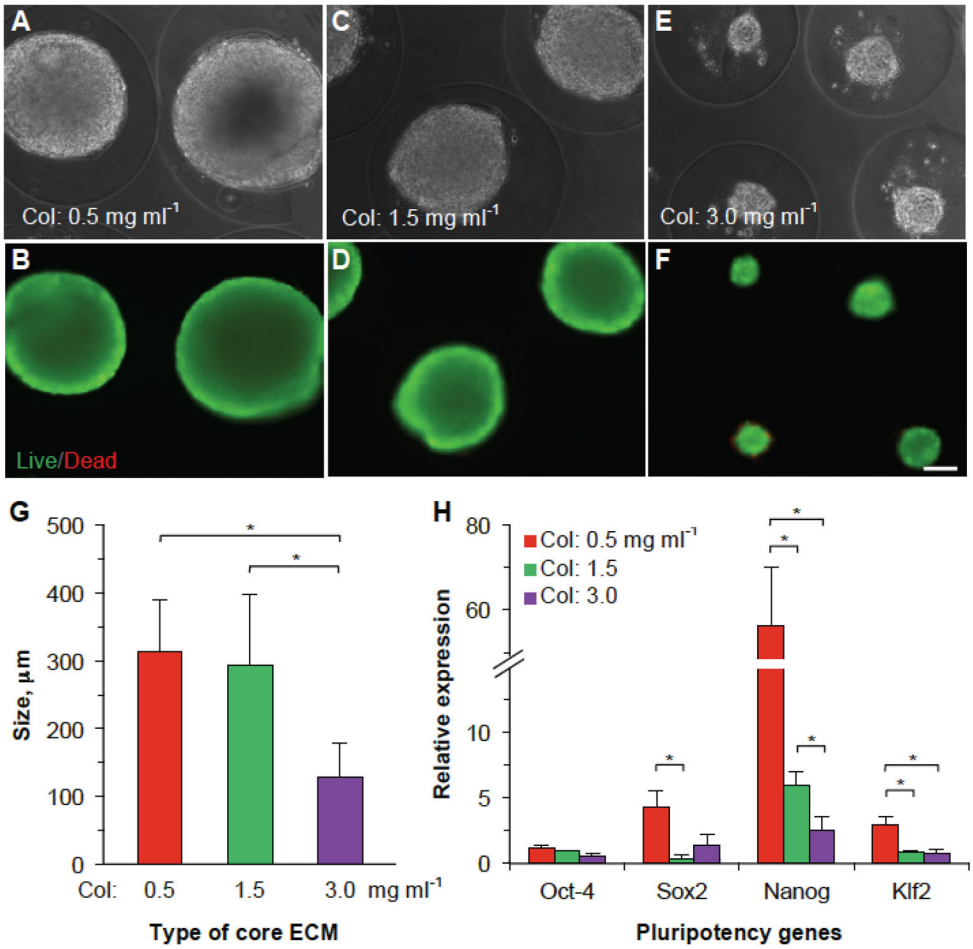

Figure 3.

Proliferation of encapsulated mESCs in different collagen core ECMs with varying structural and mechanical properties. (A–F) Phase contrast and fluorescence (live/dead) images of the mESC aggregates on day 10 in different core ECMs. Massive aggregates were formed in softer core ECM with low collagen (0.5–1.5 mg ml^{-1}) compared to significantly smaller aggregates in more rigid core with high collagen (3.0 mg ml^{-1}). (G) Quantitative data of the size of aggregates formed in microcapsules with different core ECMs. (H) Quantitative RT-PCR data showing expression of pluripotency gene markers in the aggregated mESCs obtained from different core ECMs on day 10. Col: collagen. Alg: alginate. * denotes $p < 0.05$. Scale bar: 100 µm.

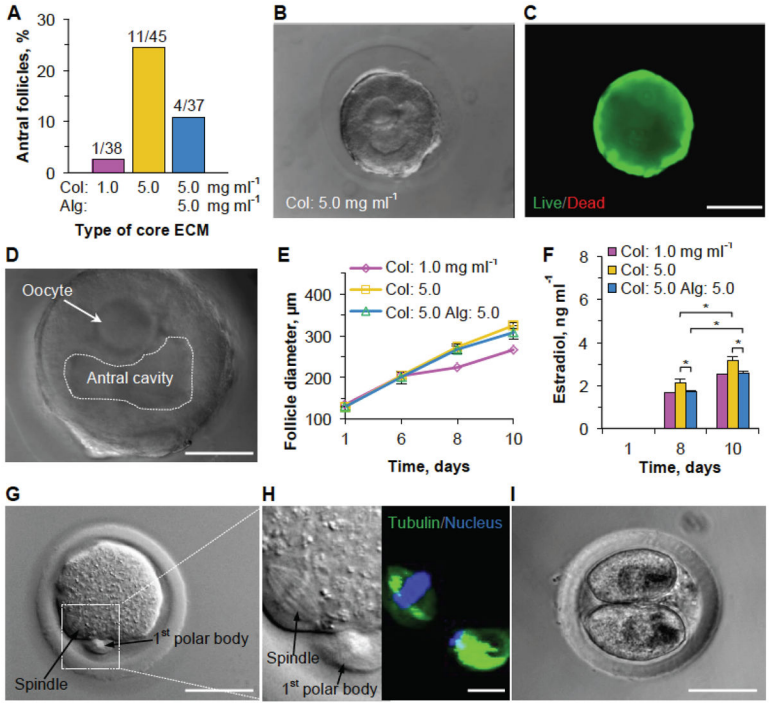

Figure 4.

Development of preantral follicles of deer mice in various core ECMs and embryo development of MII oocyte after parthenogenetic activation. (A) Quantitative data (pooled, the number of preantral follicles $n \geq 37$) showing the effect of core ECM on the development of preantral follicles to the antral stage. (B and C) Typical phase contrast and fluorescence (live/dead) images of an encapsulated follicle on day 10 when it developed to the antral stage. (D) Typical DIC image of an antral follicle (released from microcapsule) showing its characteristic fluid-filled antral cavity and an oocyte contained in cumulus-oocyte complex (COC). (E) Quantitative data showing the effect of the core ECM on the diameter of the growing follicles that developed to the antral stage on day 10. (F) Estradiol secretion on different days from the encapsulated follicles that developed to the antral stage on day 10 in different core ECMs. (G) Typical image of a metaphase II (MII) oocyte obtained from the antral follicles showing the characteristic 1st polar body and mitotic spindle of MII oocytes. (H) Hoechst and tubulin staining of the MII oocyte. (I) Image of a two-cell embryo developed from the MII oocyte after parthenogenetic activation. Col: collagen. Alg: alginate. * denotes $p < 0.05$. Scale bar: 200 µm in B and C, 50 µm in D, G, and I, and 10 µm in H.